Dependence of entanglement dynamics on the global classical dynamical regime

N. N. Chung and L. Y. Chew
Division of Physics and Applied Physics, School of Physical and Mathematical Sciences, Nanyang Technological University, 21 Nanyang Link, Singapore 637371, Singapore
(Received 16 March 2009; published 7 July 2009)

We analyze the connections between the dynamical generation of continuous variable entanglement and the underlying classical trajectories in pairs of coupled oscillators. In the quantization of a periodic cycle, we find periodic entanglement which has twice the frequency of the corresponding classical motion. Such frequency doubling continues to hold true in the entanglement dynamics for a second model that exhibits a two-frequency orbit in the classical domain. In addition, the periodicity and the quasiperiodicity of the entanglement are found to be independent of the local classical dynamical behavior. Finally, in our third model, the entanglement production rate is found to be (i) higher in the chaotic regime and (ii) insensitive toward the choice of regular or chaotic initial condition in the mixed regime. In summary, we have illustrated through our sample models that the generation of dynamical pattern of entanglement can depend completely on the global classical dynamical regime without being influenced by the local classical behavior.

DOI: 10.1103/PhysRevE.80.016204 PACS number(s): 05.45.Mt, 03.67.Mn, 03.65.Sq

I. INTRODUCTION

There has been extensive research revealing the correspondence between quantum and classical mechanics. Notable examples include the manifestation of chaos in the energy-level distribution of atomic systems, as well as the wave patterns associated with those levels. Interestingly, such correspondence can also exist within the entanglement of coupled quantum systems, whose research is especially fascinating at the regime where transition to chaos occurs. The investigation typically involves an examination into the maximal mean value and the production rate of entanglement based on nonlinear models such as the four-dimensional standard map [1], coupled kicked tops [2–8], interacting spins system [9,10] and the Jaynes-Cummings model [11], which are typical examples of finite-dimensional systems. In these studies, classical chaos is found to induce a stronger entanglement [1,11], with the entanglement production rate linked to the Lyapunov exponent [4]. In addition, they have shown that increased chaos leads to an eventual saturation of the entanglement production rate [7]. In contrast, less work has been done on entanglement in infinite-dimensional systems (also known as continuous variable entanglement) and their correspondence to classical chaos. Recently, Zhang and Jie [12] investigated the production of continuous variable entanglement through the quantization of classical tori and the mixed trajectories. They have found good quantum-classical correspondence. This has stimulated us to explore the quantum-classical correspondence in a similar context, with an additional situation of a purely chaotic regime which has yet to be explored within infinite-dimensional systems. Furthermore, we believe that interesting quantum-classical correspondence arises not only in the regime that transits to chaos, but it can also occur within the regime of regular systems. In fact, detailed studies on the dynamics of entanglement when the corresponding classical system is regular have been lacking. For example, there is no investigation yet on the quantum-classical correspondence for a system that displays periodic entanglement. Although quasiperiodic classical dynamics has been shown to correspond to entanglement dynamics with either quasiperiodicity or saturation, the underlying classical dynamics for a system that exhibits quasiperiodic entanglement dynamics is still not clear. Indeed, an interesting question that we want to answer is can a periodic classical trajectory give rise to a quasiperiodic entanglement dynamics upon quantization?

In this paper, the initial states $|\psi(0)\rangle$ are chosen to be the coherent states $|\alpha_1\rangle \otimes |\alpha_2\rangle$. This serves as the connection between the quantum and the classical domains [12]. The center of the coherent state is located precisely on a point (x_1, p_1, x_2, p_2) in the classical phase space. Note that $\alpha_l = (x_l + ip_l)/\sqrt{2}$. The dynamics of the quantum system is investigated both numerically and analytically. For numerical simulation, it is convenient to choose as basis vectors the product states $|n_1\rangle \otimes |n_2\rangle$, in which $|n_1\rangle$ and $|n_2\rangle$ are the eigenvectors of the harmonic oscillator, and we shall truncate this basis at the size M. With this basis, the Schrödinger equation becomes

$$i\hbar \frac{d}{dt}\langle m_1, m_2|\psi(t)\rangle = \sum_{n_1=0}^{M}\sum_{n_2=0}^{M}\langle m_1, m_2|H|n_1, n_2\rangle\langle n_1, n_2|\psi(t)\rangle, \tag{1}$$

where H is the Hamiltonian of the two-coupled oscillator system of interest and $\langle m_1, m_2|H|n_1, n_2\rangle$ is a four-dimensional matrix [13]. The entanglement of the time-evolved state is quantified by the von Neumann entropy (S_{vN}) of the reduced density matrix (ρ_1),

$$S_{vN}(t) = -\mathrm{Tr}\{\rho_1(t)\ln \rho_1(t)\}, \tag{2}$$

which one can compute by means of the dynamical two-step approach [14] for faster converging results. In addition, we shall introduce the quantity ξ, which is closely related to the entanglement. According to the criterion developed by Duan *et al.* [15], as long as the parameter

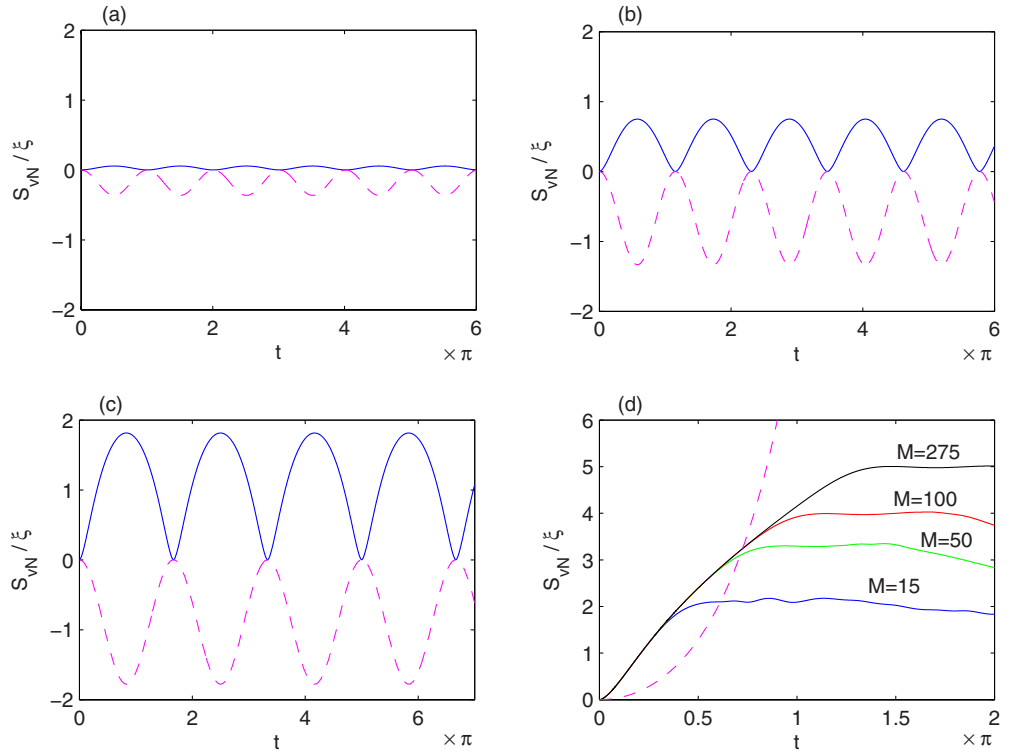

FIG. 1. (Color online) Dynamics of quantum entanglement (solid curve) and $\xi(t)$ (dashed curve) in two-mode magnon system with coupling strengths (a) $\lambda=0.1$, (b) $\lambda=0.5$, (c) $\lambda=0.8$, and (d) $\lambda=1.1$.

$$\xi = (\Delta u)^2 + (\Delta v)^2 - 2 < 0, \tag{3}$$

the quantum state is entangled. Note that $u=x_1+x_2$ and $v=p_1-p_2$ are the two Einstein-Podolsky-Rosen-type operators, while Δu and Δv are the corresponding quantum fluctuations. Analytical solutions of the quantum fluctuation in the linear models will be worked out by means of the Heisenberg equation of motion,

$$\frac{d}{dt}a_j = \frac{1}{i\hbar}[a_j, H], \tag{4}$$

with a_j being the annihilation operators.

Our paper involves a study on three conservative Hamiltonian systems and is organized as follows. In Sec. II, we show the transition of a classical fixed point from a center to a saddle point in a two-mode magnon system. The response of the quantized system to this transition is then investigated by means of the dynamical generation of quantum entanglement and fluctuation. In Sec. III, we proceed to exploring the correspondence of periodic and quasiperiodic classical trajectories in a two-coupled harmonic-oscillator system with the entanglement dynamics of their quantized counterparts. In Sec. IV, we investigate the change in entanglement dynamics as the corresponding classical dynamics transits from the regular to the chaotic regime through a coupled quartic-oscillator model. For the models discussed in these sections, we aim to seek for the correspondence, if any, between the classical trajectories within different global dynamical regimes and the continuous variable entanglement dynamics of the quantized system. Note that our main focus is on the dynamics rather than the production rate of quantum entanglement. Finally, in Sec. V, we conclude our paper.

II. TWO-MODE MAGNON SYSTEM

The Hamiltonian of our first model is given by

$$H = \frac{p_1^2}{2m} + \frac{1}{2}m\omega_0^2 x_1^2 + \frac{p_2^2}{2m} + \frac{1}{2}m\omega_0^2 x_2^2 + \lambda(x_1x_2 - p_1p_2), \tag{5}$$

where p_1 and p_2 are the kinetic momenta, x_1 and x_2 are the oscillators' positions, and λ is the coupling constant. We have assumed that $m=\omega_0=1$, and $\lambda \geq 0$. In the classical regime, $\lambda=1$ is the transition point where the fixed point at the origin transits from a center to a saddle—i.e., trajectories cycle with a frequency of $\omega=\sqrt{1-\lambda^2}$ around the origin when $\lambda<1$ but evolve either toward or away from the origin when $\lambda>1$.

The second quantization of Eq. (5) gives the following Hamiltonian:

$$H = \hbar\left(a_1^\dagger a_1 + \tfrac{1}{2}\right) + \hbar\left(a_2^\dagger a_2 + \tfrac{1}{2}\right) + \lambda\hbar(a_1^\dagger a_2^\dagger + a_1 a_2), \tag{6}$$

which models the two-mode magnons excited by an external field [16]. Note that $x_j=\sqrt{\hbar}(a_j^\dagger+a_j)/\sqrt{2}$ and $p_j=\sqrt{\hbar}(a_j^\dagger - a_j)/(\sqrt{2}i)$. For the quantized system, we determine the entanglement dynamics numerically from several initial coherent states for $\lambda=0.1$, 0.5, and 0.8 with a basis size of $M=50$. The resultant entanglement dynamics is found to depend only on the coupling strength λ but not on the initial

coherent state. Figures 1(a)–1(c) show that the entanglement dynamics is periodic when $\lambda < 1$. Interestingly, the periods of entanglement dynamics are exactly half the periods of the corresponding classical motions. This frequency-doubling phenomenon in the quantization of the classical periodic orbit has been reported earlier by Satchell and Sarben [17] for quantum moment in a dissipative system. Our result here and in the next section shows that this phenomenon remains true in a conservative system.

By increasing λ, we observe an increase in the maximum attainable entanglement. This means that the stronger the interaction between the two modes, the more they become entangled. Figure 1(d) shows the entropy dynamics at different basis sizes in the saddle regime, where we simulate the entanglement dynamics with $\lambda = 1.1$. As time goes on, we observe that the number of basis required to approximate the time-evolved state increases rapidly. It seems that the strong interaction between the two modes has induced a rapid growth in the entropy as the quantized system crosses the $\lambda = 1$ transition point.

Next, we determine the time-dependent equation of the ladder operators $a_j(t)$ and $a_j^\dagger(t)$ for $j = 1, 2$ by means of the Heisenberg formulation of quantum mechanics,

$$\frac{d}{dt}\begin{pmatrix} a_1 \\ a_2^\dagger \end{pmatrix} = \begin{pmatrix} -i & -i\lambda \\ i\lambda & i \end{pmatrix}\begin{pmatrix} a_1 \\ a_2^\dagger \end{pmatrix}, \tag{7}$$

whose solutions are given by

$$a_1(t) = \left[\cosh(\kappa t) - \frac{i}{\kappa}\sinh(\kappa t)\right]a_1(0) - \frac{i\lambda}{\kappa}\sinh(\kappa t)a_2^\dagger, \tag{8}$$

$$a_2^\dagger(t) = \left[\cosh(\kappa t) + \frac{i}{\kappa}\sinh(\kappa t)\right]a_2^\dagger(0) + \frac{i\lambda}{\kappa}\sinh(\kappa t)a_1, \tag{9}$$

where $\kappa = \sqrt{\lambda^2 - 1}$. The time dependence of ξ is given by

$$\xi(t) = 2(\langle a_1^\dagger a_1\rangle - \langle a_1^\dagger\rangle\langle a_1\rangle + \langle a_2^\dagger a_2\rangle - \langle a_2^\dagger\rangle\langle a_2\rangle + \langle a_1^\dagger a_2^\dagger\rangle - \langle a_1^\dagger\rangle\langle a_2^\dagger\rangle + \langle a_1 a_2\rangle - \langle a_1\rangle\langle a_2\rangle), \tag{10}$$

where $\langle O\rangle$ in Eq. (10) means $\langle \alpha_1, \alpha_2|O(t)|\alpha_1, \alpha_2\rangle$. Substituting Eqs. (8) and (9) and their conjugates into Eq. (10), we obtain

$$\xi(t) = \frac{4\lambda}{|\lambda^2 - 1|}(\lambda - 1)|\sinh(t\sqrt{\lambda^2 - 1})|^2. \tag{11}$$

For $\lambda < 1$, we have

$$\xi(t) = \frac{2\lambda}{\lambda + 1}\{\cos(2t\sqrt{1 - \lambda^2}) - 1\}, \tag{12}$$

which is always less than the lower bound—zero. According to Duan's criterion, the violation of the lower bound serves as a sufficient condition for entanglement. This analysis through Duan's criterion corresponds to our numerical quantification based on the von Neumann entropy. First, the sum of quantum fluctuations is independent of the chosen initial coherent state ($|\alpha_1\rangle \otimes |\alpha_2\rangle$) as shown in Eqs. (11) and (12), just like our conjecture on the entropy dynamics. This can be observed from the value of $\xi(t)$, which depends only on λ. Thus, the entanglement dynamics of the two-mode magnon system is independent of the local classical behavior. Next, the periodic $\xi(t)$ has a frequency of $2\sqrt{1-\lambda^2}$, which is exactly twice the corresponding classical frequency. It is important to note that $\xi(t)$ is always greater than zero when $\lambda > 1$. As a sufficient but not a necessary criterion, Duan's criterion can no longer determine whether the state is entangled or separable in the $\lambda > 1$ regime. Nonetheless, the analytical result for $\xi(t)$ does show a transition point at $\lambda = 1$. Indeed, $\xi(t)$ diverges to infinity for $\lambda \geq 1$, in direct correspondence to the fact that the entanglement between the two oscillators grows rapidly in time. Finally, these results illustrate the good quantum-classical correspondence in the bifurcation behavior [18] of the two-mode magnon system, which exemplifies the manner in which entanglement dynamics can depend on the global classical dynamical regime.

III. COUPLED HARMONIC OSCILLATORS

The Hamiltonian of our second model involves two harmonic oscillators coupled in a bilinear fashion,

$$H = \frac{p_1^2}{2m} + \frac{1}{2}m\omega_0^2 x_1^2 + \frac{p_2^2}{2m} + \frac{1}{2}m\omega_0^2 x_2^2 + \lambda x_1 x_2. \tag{13}$$

Physical realizations of such systems include vibrating molecules and modes of the electromagnetic field [19,20]. Again, we have set $m = \omega_0 = 1$. Furthermore, we have restricted $\lambda < 1$. In general, the classical trajectories yield two-frequency ($\omega_{1,2} = \sqrt{1 \pm \lambda}$) periodic or quasiperiodic orbits, provided the initial conditions are not in the eigenspace of either one of the frequencies. For instance, when $\lambda = 11/61$, the classical trajectory has a rational ratio of frequency and is hence periodic. On the other hand, when $\lambda = 0.19$, the classical trajectory consists of two incommensurate frequencies and is quasiperiodic. The Poincaré sections for these two cases are shown in Figs. 2(a) and 2(c). Note that the crosses represent one-frequency periodic orbits when the initial conditions lie in the eigenspace, while the sets of points and the closed curves correspond to two-frequency periodic and quasiperiodic orbits, respectively.

The second-quantized form of Eq. (13) is given as follows:

$$H = \hbar\left(a_1^\dagger a_1 + \frac{1}{2}\right) + \hbar\left(a_2^\dagger a_2 + \frac{1}{2}\right) + \frac{\lambda\hbar}{2}(a_1^\dagger + a_1)(a_2^\dagger + a_2). \tag{14}$$

Figures 2(b) and 2(d) show the numerical results of the entropy dynamics for $\lambda = 11/61 \approx 0.18$ and 0.19, respectively. Although the value of the maximum entropy for these two cases are closed to each other, the entanglement possesses very different dynamics—periodic for the former and quasiperiodic for the latter within the time of 40π.

We next solve the Heisenberg equation of motion for this two-coupled harmonic-oscillator system as follows:

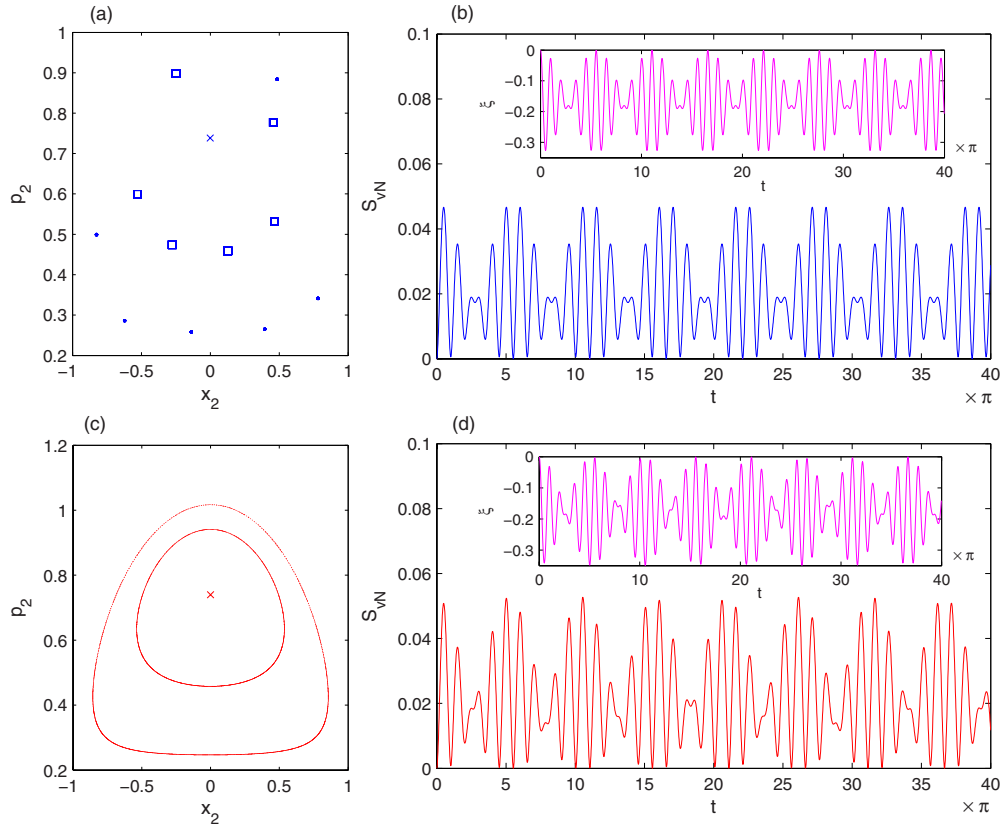

FIG. 2. (Color online) Poincaré surface of section and entanglement dynamics of the coupled harmonic-oscillator system: $\lambda=11/61$ for (a) and (b), while $\lambda=0.19$ for (c) and (d). Insets in (b) and (d) show the corresponding dynamics of $\xi(t)$.

$$\frac{d}{dt}\begin{pmatrix} a_1 \\ a_1^\dagger \\ a_2 \\ a_2^\dagger \end{pmatrix} = \begin{pmatrix} -i & 0 & -i\frac{\lambda}{2} & -i\frac{\lambda}{2} \\ 0 & i & i\frac{\lambda}{2} & i\frac{\lambda}{2} \\ -i\frac{\lambda}{2} & -i\frac{\lambda}{2} & -i & 0 \\ i\frac{\lambda}{2} & i\frac{\lambda}{2} & 0 & i \end{pmatrix}\begin{pmatrix} a_1 \\ a_1^\dagger \\ a_2 \\ a_2^\dagger \end{pmatrix} \tag{15}$$

and obtain

$$a_1(t) = (-A_1 + B_1 - A_2 + B_2)a_1(0) - (C_1 + C_2)a_1^\dagger(0) + (-A_1 + B_1 + A_2 - B_2)a_2(0) - (C_1 - C_2)a_2^\dagger(0), \tag{16}$$

$$a_2^\dagger(t) = -(C_1^* - C_2^*)a_1(0) + (B_1^* - A_1^* - B_2^* + A_2^*)a_1^\dagger(0) - (C_1^* + C_2^*)a_2(0) + (B_1^* - A_1^* + B_2^* - A_2^*)a_2^\dagger(0), \tag{17}$$

where

$$A_{1,2} = \frac{(\omega_{1,2}-1)^2}{8\omega_{1,2}}e^{i\omega_{1,2}t},$$

$$B_{1,2} = \frac{(\omega_{1,2}+1)^2}{8\omega_{1,2}}e^{-i\omega_{1,2}t},$$

$$C_{1,2} = \frac{2i(\omega_{1,2}-1)(\omega_{1,2}+1)}{8\omega_{1,2}}\sin(\omega_{1,2}t).$$

This solution enables us to determine the dynamics of the sum of quantum fluctuations which gives

$$\xi(t) = -\frac{1}{2}\frac{\omega_1^2-1}{\omega_1^2}[1-\cos(2\omega_1 t)] + \frac{1}{2}(\omega_2^2-1)[1-\cos(2\omega_2 t)]. \tag{18}$$

Interestingly, the analytical result is in accordance with our numerical result—there is also a two-frequency dynamics in the sum of quantum fluctuations. The two frequencies, $\Omega_1=2\sqrt{1+\lambda}$ and $\Omega_2=2\sqrt{1-\lambda}$, are twice the corresponding classical frequencies ω_1 and ω_2, respectively, which is again the frequency-doubling scenario that we have obtained in our first model. Furthermore, the dynamics, which is either periodic or quasiperiodic, depends on the ratio of the two frequencies Ω_1/Ω_2, instead of the local dynamical behavior of the underlying classical trajectories. This is because both the entanglement and the sum of quantum fluctuations depend only on the coupling strength and not on the chosen initial coherent state. Thus, the entanglement dynamics of the coupled harmonic oscillators is dependent solely on the global classical behavior. The most dramatic effect of this global

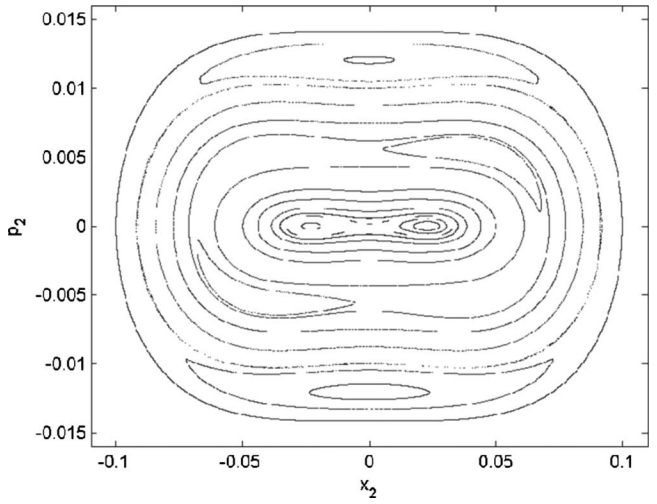

FIG. 3. Classical phase portrait for the coupled quartic-oscillator system with coupling constant $\lambda=0.4$.

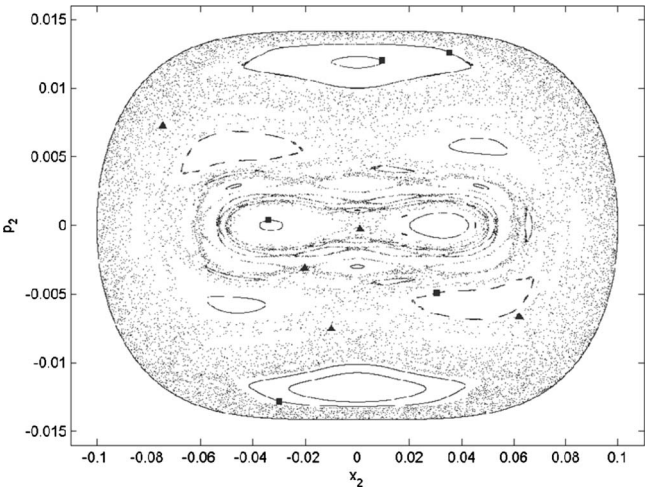

FIG. 4. Classical phase portrait for the coupled quartic-oscillator system with coupling constant $\lambda=0.8$. Note that the marked points indicate the coherent states employed as initial conditions in the dynamical evolution.

dependence is observed for the quasiperiodic entanglement dynamics of Fig. 2(d), which corresponds to the classical periodic orbit indicated by a cross in Fig. 2(c). This indicates that a periodic classical trajectory can give rise to a quasiperiodic entanglement dynamics upon quantization, answering the question posed in Sec. I. Indeed, similar counterintuitive influence of the global classical dynamical regime applies to the one-frequency periodic orbit (indicated by a cross) in Fig. 2(a), which corresponds to a two-frequency periodic entanglement dynamics as illustrated in Fig. 2(b).

IV. COUPLED QUARTIC OSCILLATORS

The classical dynamics of the coupled quartic-oscillator system based on the following Hamiltonian:

$$H=\tfrac{1}{2}(p_1^2+p_2^2)+3x_1^4+x_2^4-\lambda x_1^2x_2^2 \tag{19}$$

has been found to range from regular behavior to completely chaotic behavior through the variation in the coupling constant λ. It is observed that the system becomes more chaotic as the coupling becomes larger. For instance, the phase space is a mixture of classical tori and chaotic sea when $\lambda=0.8$ but becomes purely chaotic when $\lambda=2.7$. Figures 3–5 show the respective phase portraits of classically regular, mixed, and chaotic dynamics for this system. Note that good quantum-classical correspondence has been found in the study of the quantum energy-level distribution of this system [21].

In order to treat the quantum and the classical regimes with care, we adopt the parameter $R=\hbar/\Lambda$ to quantify the "quantumness" of the system [22]. Note that $\Lambda=|\alpha_1|^2+|\alpha_2|^2$ is the action of the system with α_1 and α_2 being the coordinates of the coherent state. When $R\gg 1$, the system is in the quantum regime. On the other hand, when $R\ll 1$, the system is in the semiclassical regime. The semiclassical regime can be approached in either of the two ways: $\hbar\to 0$ or $\Lambda\to\infty$. The latter case corresponds to the high-energy approximation in the semiclassical theory. The former case is the one adopted in this paper.

By first considering the quantum regime with $R\gg 1$, we simulate the entropy dynamics of the quantized system of Eq. (19) at $\lambda=0.4$, 0.8, and 2.7. The results are shown in Fig. 6. Next, we treat the system semiclassically with $R<0.1$, for which we again simulate the entropy dynamics of the quantized system of Eq. (19) at $\lambda=0.4$, 0.8, and 2.7. The results are shown in Fig. 7. Compared to the quantum treatment, the entropy of entanglement is much larger in the semiclassical regime. Nevertheless, similar phenomena are observed to occur in the two regimes. First, in both treatments, the entanglement production rate is the highest for the case of pure chaos, lower for the mixed case, and the lowest for the regular case, in correspondence to the finite-dimensional systems [11,1]. Second, the frequency of the oscillation becomes higher as λ becomes larger. Finally, identical results are obtained in the mixed case even though the entanglement dynamics is simulated numerically from different initial coherent states. This indicates that the entanglement dynamics is

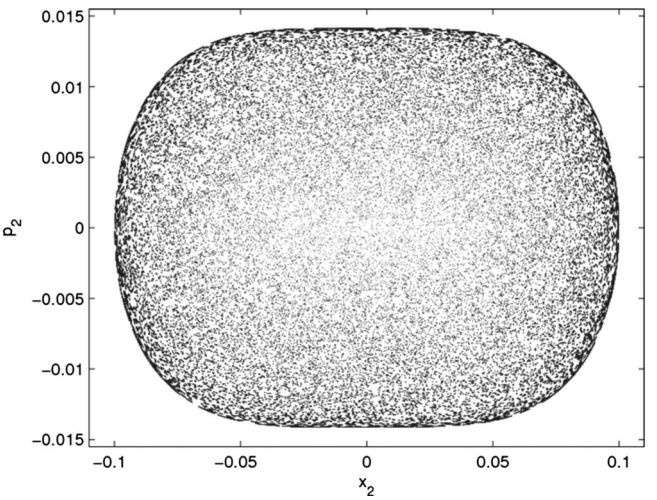

FIG. 5. Classical phase portrait for the coupled quartic-oscillator system with coupling constant $\lambda=2.7$.

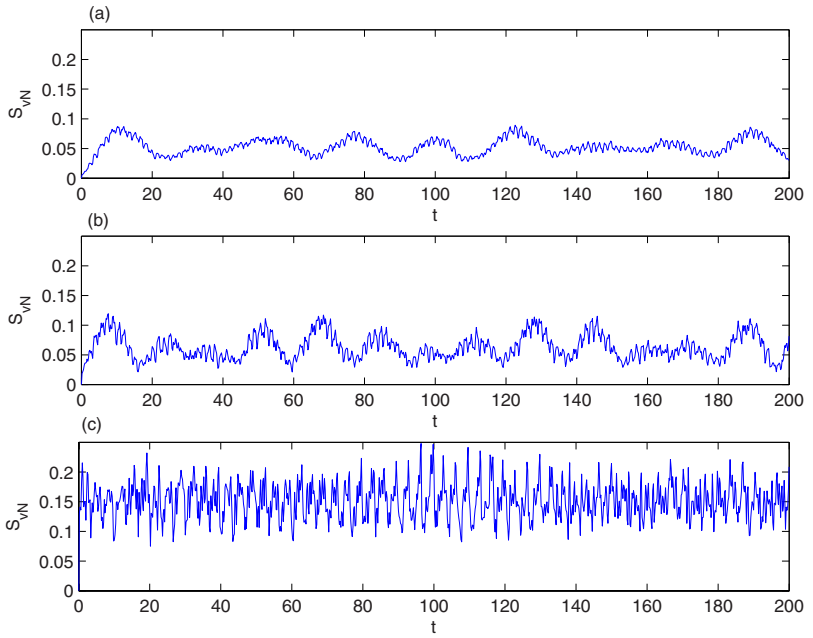

FIG. 6. (Color online) Entanglement dynamics for the coupled quartic-oscillator system with coupling constants (a) $\lambda=0.4$, (b) $\lambda=0.8$, and (c) $\lambda=2.7$ in the quantum regime.

insensitive toward the choice of regular or chaotic initial condition in the mixed case for a fixed energy. In other words, the behavior of the entanglement dynamics in this model depends entirely on the global classical dynamical regime and not on the local classical behavior. This is quite a surprising result, which is different from those obtained by Zhang and Jie [12] for an infinite-dimensional system and Novaes [10] for a finite-dimensional system. They have both observed a local influence of the classical regular and chaotic dynamics on the corresponding entanglement dynamical pattern. In Fig. 8, we have reproduced the dependence of the entanglement production on the classical tori observed by Zhang and Jie to show the obvious difference from our case.

V. CONCLUSION

We have explored the link between classical trajectories and continuous variable entanglement dynamics in three pairs of two-coupled oscillator system. In the first model, the quantization of periodic orbits yields periodic entanglement, whereas the quantization of saddle produces a rapid growth of entropy, with the transition occurring at $\lambda=1$ for both the classical and the quantum regimes. For the second model, the quantization of periodic orbits in the case of commensurate frequencies has led to periodic entanglement dynamics, while the quantization of both the periodic orbit and the quasiperiodic tori in the case of incommensurate frequencies has

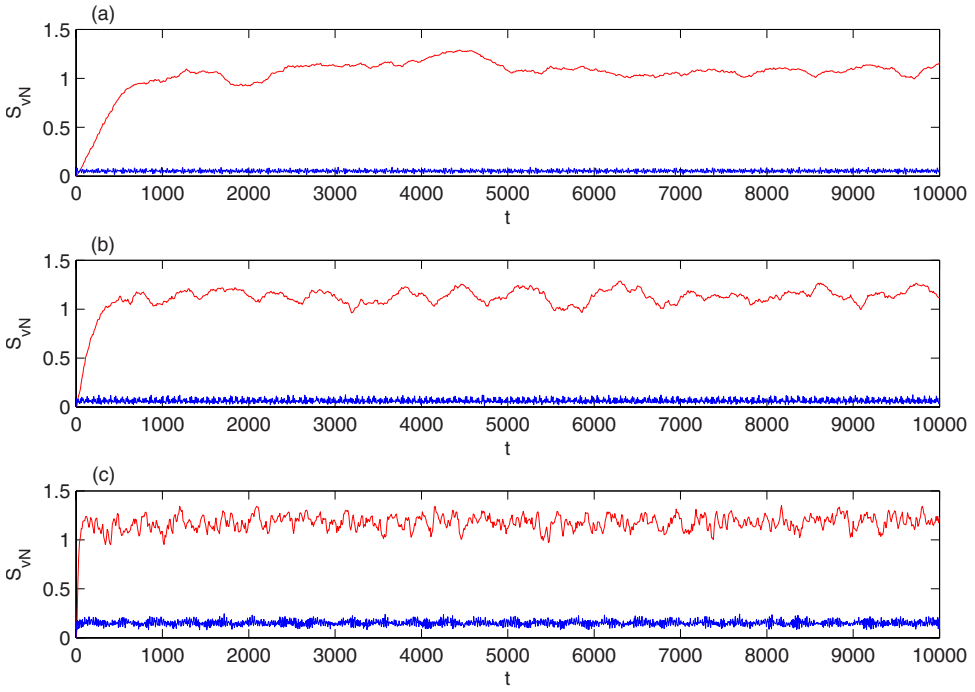

FIG. 7. (Color online) Entanglement dynamics for the coupled quartic-oscillator system with coupling constants (a) $\lambda=0.4$, (b) $\lambda=0.8$, and (c) $\lambda=2.7$. The upper curves show results from the semiclassical treatment whereas the lower curves show results in the quantum regime.

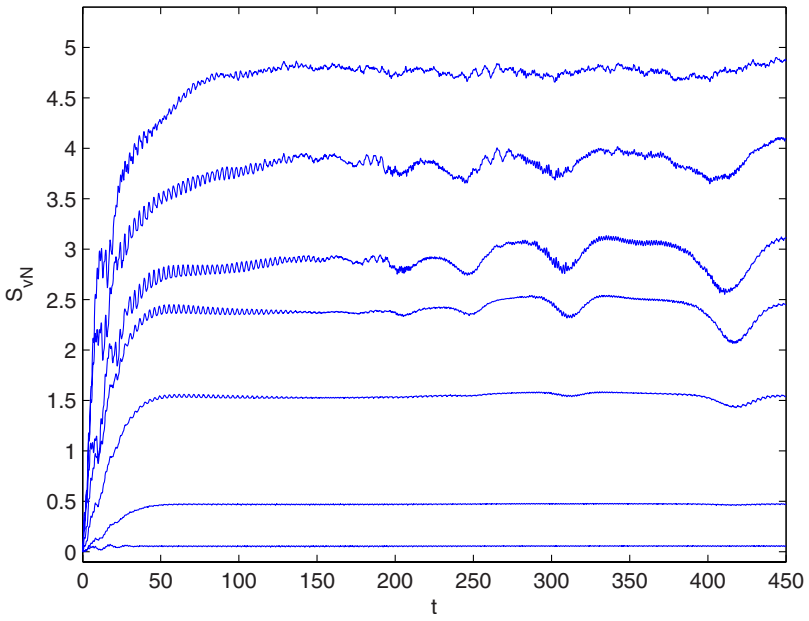

FIG. 8. (Color online) Entanglement dynamics simulated from seven initial coherent states for a harmonic-oscillator pair coupled by biquadratic potential (see [12]). Note that the von Neumann entropy shown here has been multiplied by a factor of $1/\ln 2$, so that the definition of von Neumann entropy is the same as that used in [12].

led to quasiperiodic entanglement dynamics. Interestingly, the dynamical feature of the entanglement dynamics is solely parametrized by the two independent frequencies of the classical system. In the third model, the quantization of either the regular, the mixed, or the chaotic regime of a coupled quartic oscillators yield entanglement dynamics that are again independent of the classical initial conditions, just like the first two models. This is unexpected as entanglement is generally known to depend on local dynamical behavior [10] and structure of the classical phase space [23], as well as nonclassical features such as the type of initial states [8] and their spectral widths [24], for nonlinear systems. In conclusion, we have found that entanglement dynamics can be dependent on the global classical dynamical regime but independent of the local classical behavior in both integrable and nonintegrable models. With entanglement being an important resource in quantum communication and computation, we would expect these "nonlocal" models to generate an encoding subspace [25] that is stable against any errors in the preparation of the initial separable coherent states. Such a feature will be physically significant in the design of robust quantum information processing protocols.

[1] A. Lakshminarayan, Phys. Rev. E **64**, 036207 (2001).
[2] J. N. Bandyopadhyay and A. Lakshminarayan, Phys. Rev. Lett. **89**, 060402 (2002).
[3] J. N. Bandyopadhyay and A. Lakshminarayan, Phys. Rev. E **69**, 016201 (2004).
[4] P. A. Miller and S. Sarkar, Phys. Rev. E **60**, 1542 (1999).
[5] H. Kubotani, S. Adachi, and M. Toda, Phys. Rev. Lett. **100**, 240501 (2008).
[6] X. G. Wang, S. Ghose, B. C. Sanders, and B. Hu, Phys. Rev. E **70**, 016217 (2004).
[7] H. Fujisaki, T. Miyadera, and A. Tanaka, Phys. Rev. E **67**, 066201 (2003).
[8] R. Demkowicz-Dobrzanski and M. Kus, Phys. Rev. E **70**, 066216 (2004).
[9] C. Mejia-Monasterio, G. Benenti, G. G. Carlo, and G. Casati, Phys. Rev. A **71**, 062324 (2005).
[10] M. Novaes, Ann. Phys. (N.Y.) **318**, 308 (2005).
[11] K. Furuya, M. C. Nemes, and G. Q. Pellegrino, Phys. Rev. Lett. **80**, 5524 (1998).
[12] S.-H. Zhang and Q.-L. Jie, Phys. Rev. A **77**, 012312 (2008).
[13] N. N. Chung and L. Y. Chew, Phys. Rev. A **76**, 032113 (2007).
[14] N. N. Chung and L. Y. Chew, Phys. Rev. A **80**, 012103 (2009).
[15] L. M. Duan, G. Giedke, J. I. Cirac, and P. Zoller, Phys. Rev. Lett. **84**, 2722 (2000).
[16] F. Peng, EPL **54**, 688 (2001).
[17] J. S. Satchell and S. Sarben, J. Phys. A **19**, 2737 (1986).
[18] X. W. Hou, J. H. Chen, and B. Hu, Phys. Rev. A **71**, 034302 (2005).
[19] D. A. Parshin and C. Laermans, Physica B **316-317**, 542 (2002).
[20] S. Ikeda and F. Fillaux, Phys. Rev. B **59**, 4134 (1999).
[21] M. Tomiya, N. Yoshinaga, S. Sakamoto, and A. Hirai, Comput. Phys. Commun. **169**, 313 (2005).
[22] L. Sanz, R. M. Angelo, and K. Furuya, J. Phys. A **36**, 9737 (2003).
[23] M. Lombardi and A. Matzkin, Phys. Rev. A **73**, 062335 (2006).
[24] T. Gorin and T. H. Seligman, Phys. Lett. A **309**, 61 (2003).
[25] E. Ciancio and P. Zanardi, Phys. Lett. A **360**, 49 (2006).